



## IMPEDANCE SPECTROSCOPY OF POLYMER-CERAMIC COMPOSITES

H. S. Aliyev, H. V. Fattayev

*Azerbaijan Technical University, Baku, Azerbaijan*

### ABSTRACT

Polymer-ceramic composites from a new class of construction and functional materials of great potential applications in having combined hardness and stiffness of ceramics along with flexibility, elasticity, low density, and higher breakdown strength of polymers and hence are being increasingly harnessed for their specific dielectric, ferroelectric, piezoelectric, piezoelectric, electro-optic, as well as superconducting properties in micro-devices. The charge transport mechanism in polymer-ceramic composites is a longstanding problem. Alternating Current Impedance Spectroscopy (ACIS) is found to be a valuable experimental tool for the understanding of the phenomenon of the charge transport in micro-and nano composites.

### KEYWORDS

Polymer composite;  
Impedance spectroscopy;  
Polymer;  
Complex resistance;  
Electric field;  
Relaxation time;  
Phase shift angle.

© 2022 «OilGasScientificResearchProject» Institute. All rights reserved.

### 1. Introduction

The presence of volume charge on a polymer material with a highly heterogeneous structure (for example, a composite) leads to the formation of various effects characterized by quasi-equilibrium. This is most likely due to the fact that polymers are able to hold charges due to the presence of localized levels in the quasi-blocking zone.

The formation of internal microdischarges, electric, piezoelectric, and pyroelectric effects during treatment of polymers by strong electric fields, discharges, and mechanical influences at different temperatures (including cryogenic ones) is considered as an example of quasi-equilibrium.

Identification of peculiarities of carrier injection from discharge channels into a polymer requires a more detailed study of the mechanism of discharge development in the dielectric-gas-dielectric system, dielectric properties, and gas medium pressure. In all the above examples, the formation of the volume charge and its change depending on the heterogeneity of the polymer structure and external influences play a role both in the process itself and in the electrophysical properties of polymers used as passive (insulating) and active elements.

It should be noted that one of the informative methods for determining the correlation between the structure of a composite and its macroscopic properties (in addition to thermal activation spectroscopy) is the method of impedance spectroscopy [1,2].

Using this method, one can determine and analyze the dielectric and electric conductive characteristics of materials, obtain information on the transport of carriers taking into account its real microstructure, describe the volume of

particles in their conductivity, the qualitative and quantitative role in the interface, take into account the influence of the Maxwell-Wagner effects characteristic of heterogeneous structures.

### 2. Research method

This work presents preliminary results of studying the impedance spectroscopy of a composite system of various concentrations of HDPE + PKR-3M, obtained by hot pressing from a homogeneous mixture of high-density polyethylene (HDPE) and PKR-3M (PbTiO<sub>3</sub>-PbZnO<sub>3</sub>-PbNb<sub>2/3</sub>Zn<sub>1/3</sub>O<sub>3</sub>-MnO<sub>2</sub>) piezoceramic powder.

Obtaining samples for research includes the following steps:

- Matrices and filler powders are sieved to obtain appropriate dispersions;
- The components are mixed in porcelain dishes until a homogeneous mixture is obtained;
- Samples with a thickness of  $h \sim 200\mu$  and a diameter of  $d = 30$  mm are obtained from this mixture, keeping it at a temperature of 373 K and a pressure of 15 MPa for 5 minutes.

In the former case, PKR-3M powder in the desired amount was mixed thoroughly with the HDPE and F2-ME powders in an agate pestle mortar for 1h. This process coated the PKR-3M powder on the surface of the HDPE and F2-ME particles, so it referred to as prevocalization of the PKR-3M phase. Prolonged mixing improved the homogeneity of the spatial distribution of the filler particles and their uniform coating thickness on the HDPE and F2-ME particles. The tumble mixed personalized powders were prepared for different PKR-3M contents of 5-10 vol. %. The resultant powder was dried at 1000C for 6h prior to compression molding. Then, the HDPE/PKR-3M and F2-ME/PKR-3M composites prepared by hot pressing the powder mixture technique. The dried

\*E-mail: hikmetaliyev@aztu.edu.az

<http://dx.doi.org/10.5510/OGP2022SI100689>

powder was filled in a tool steel die having diameter 30 mm. the powder was heated at an average heating rate of at 60 C<sub>min</sub>/under pressure of 15 MPa to a maximum temperature. After soaking period of 10 minutes, the disk samples of 30 mm diameter and thickness 200μ were punched from the plates and cooled to 0 °C in a water – ice mixture (quenching mode) at atmospheric pressure to eliminate porosity, dabbles or blisters. Thus the 0-3 composites containing 5-10 vol. % PKR-3M in the HDPE and F2ME matrix were prepared. The specimens were sealed in air free polyethylene bags prior to measurements to avoid atmospheric and humidity effects that may induce same changes in the conductivity of the specimens.

Small amplitude of sinusoidal (AC) signal is applied to perturb the system and the frequency response recorded as impedance and phase angle. The applied potential is given by:

$$V = V_0 e^{i\omega t} \quad (1)$$

The output current of the system is represented by:

$$J = J_0 e^{i(\omega t + \varphi)}, \quad (2)$$

where,  $\omega = 2\pi f$ . According to Ohm's law the complex impedance ( $Z^*$ ) of the circuit at any frequency  $f$  can be presented by:

$$Z^* = Y_0 / J_1 = (Y / J_0)^{-i\varphi} = Z_0 e^{-i\varphi} = Z \cos \varphi - i Z \sin \varphi = Z' - Z'', \quad (3)$$

where,  $Z'$  and  $Z''$  are real and imaginary parts of the complex impedance, respectively, given as the

$$\begin{aligned} Z' &= Z \cos \varphi \\ Z'' &= Z \sin \varphi \end{aligned} \quad (4)$$

with phase angle ( $\varphi$ )

$$\varphi = \tan^{-1}(Z'' / Z') \quad (5)$$

we recognize that besides impedance  $Z^*$ , permittivity  $\varepsilon^*$  is a central quantity is shown in  $E_q$  (5)

$$C^* = \varepsilon^* C_0 = C^* = \varepsilon_0 \varepsilon^* A / \theta$$

where  $A$  – capacitors area and  $\theta$  – thickness. It follows according to  $E_q$  (5):  $Z' \sim \varepsilon'$  and  $Z'' \sim \varepsilon''$ . Hence,  $\varepsilon'$  gives the stored energy and  $\varepsilon''$  gives the dissipated energy for conductivity. We note, impedance is the key quantity of impedance spectroscopy. Interpretation of impedance reads:

- $Z'$  – represents Ohmic resistance;
- $Z''$  – can be seen as non-Ohmic resistance.

It displays characteristic frequencies especially, for dipole relaxation resulting from local motions of charged entities.

The composite preparation mode made it possible to obtain reproducible electrophysical parameters (electric resistance, capacitance, dielectric losses and figure of merit) for most of the samples at an identical concentration. Some samples with parameters differing from those of the main group were not taken into account in the analysis (the number of these samples was small). It was assumed that the filler was uniformly distributed in the composite.

It should be noted that the study of HDPE + PKR-3M composites of the «sandwich» type in the form of a capacitor was carried out in a measuring chamber, screened and connected to the ground with a value of the measuring voltage  $U = 1V$  in the frequency range (25-106) Hz. The samples were placed in a measuring cell with pressure-exerting stainless steel electrodes. The electrodes were centered with a special

mandrel in a heated chamber. The interelectrode spacing was determined by the thickness of the test samples. The impedance  $|Z|$  of composites were measured in a direction perpendicular to the compression plane of the samples.

The measurements were carried out at a frequency of 1 kHz. The test samples are placed between stainless steel electrodes. The temperature was controlled using an MMX-400 electronic thermostat. E7-20 broadband immittance meters were used for measurements.

In the experiments, the absolute value of the impedance  $|Z|(f)$  of the total complex resistance and the phase angle  $\varphi(f)$  between current and voltage were measured. Then  $Z'(f) = |Z|(f) \cdot \cos \varphi(f)$  and  $|Z''(f)| = |Z|(f) \cdot \sin \varphi(f)$ , respectively, the spectra of the real and imaginary parts of the complex impedance were calculated.

These measurements make it possible to determine and analyze the nature of the electrophysical properties of the samples under study. The relative error in measuring the impedance did not exceed 5%.

In figure 1(a) shows the dependences of the real ( $Z'$ ) and imaginary ( $Z''$ ) parts of the complex impedance on the frequency of the external electric field. As can be seen from the figure, both ( $Z'$ ) and ( $Z''$ ) sharply decrease with increasing frequency. (The rate of decreasing  $Z''$  is very fast compared to  $Z'$ ).

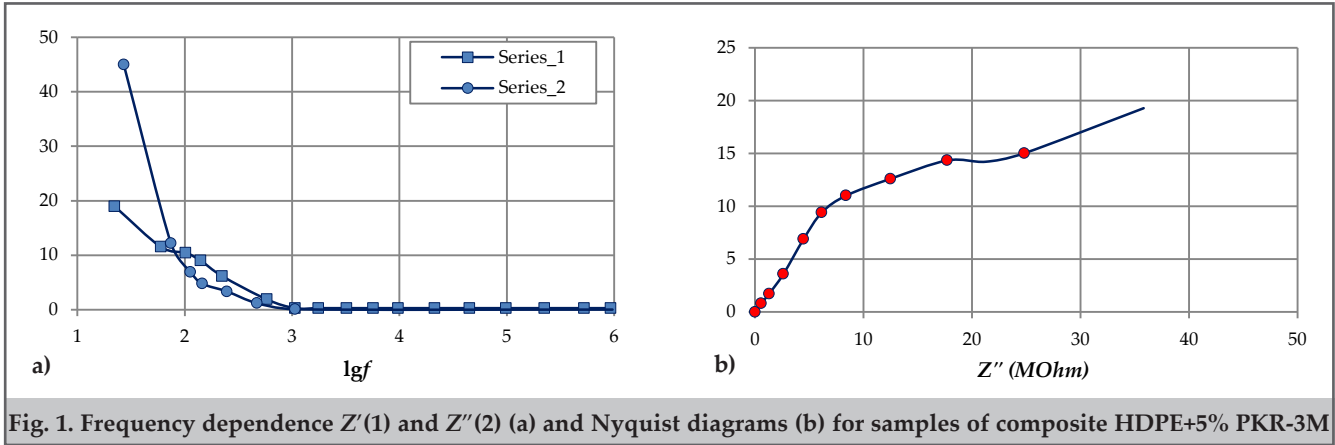
It should be noted that the increase in impedance in the low-frequency range ( $f < 500$  Hz) is due to the displacement of positive and negative charges towards the opposite electrodes and the formation of a thin layer near the electrodes, which is characterized by a high electrical capacitance.

Thus, the measurement of the impedance of polymer composites in different frequency ranges makes it possible to distinguish the processes that determine the current flowing through the sample with respect to the electrode (surface) and volumetric phenomena, as well as to determine the important electrophysical characteristics of the object (composite) under study.

To select the equivalent circuit of the studied composites and determine the optimal values of the circuit elements, the impedance spectra  $Z(f)$  obtained in practice are presented in the form of impedance hodographs (Nyquist diagrams) plotted in the coordinates of its  $Z'$  real and  $Z''$  imaginary components. It is clear that each point on the hodograph curve represents the real and imaginary components of the impedance measured at a certain frequency of the investigated frequency range.

Figure 1 (b) shows a Nyquist diagram for a composite HDPE + 5% PKR-3M sample. The plot of dependence  $Z'' = f(Z')$  has the shape of an arc at high frequencies and a linear section at low frequencies. The frequency corresponding to the maximum value of  $Z''$  in the hodograph semicircle is the relaxation frequency of the measuring rod together with the sample, and from its value it is possible to calculate the relaxation time  $\tau_x = 12 / \pi f$ , which characterizes the relaxation of the material molecules.

For HDPE+5% PKR-3M composite samples obtained by hot pressing, the frequency dependences of the real and imaginary parts of the total complex impedance  $Z' = |Z| \cdot \cos \varphi$  and  $Z'' = |Z| \cdot \sin \varphi$  and phase shift between current and voltage. According to the dependence  $Z'' = f(Z')$  on the Nyquist diagram, the characteristic relaxation time is calculated from the value of the frequency corresponding to



the maximum  $Z''$  and is  $\tau_r \approx 5,31 \cdot 10^{-3}$  sec.

Figure 2 shows the frequency dependences of the parameters  $Z'$  and  $Z''(2a)$  and Nyquist diagrams for samples of the composite F2ME and F2-ME +10% PKR-3M.

As can be seen, the nature of these dependences is similar to the dependences for HDPE and HDPE/PKR-3M composites;  $Z'' = f(Z')$  Nyquist diagrams are arc-shaped at

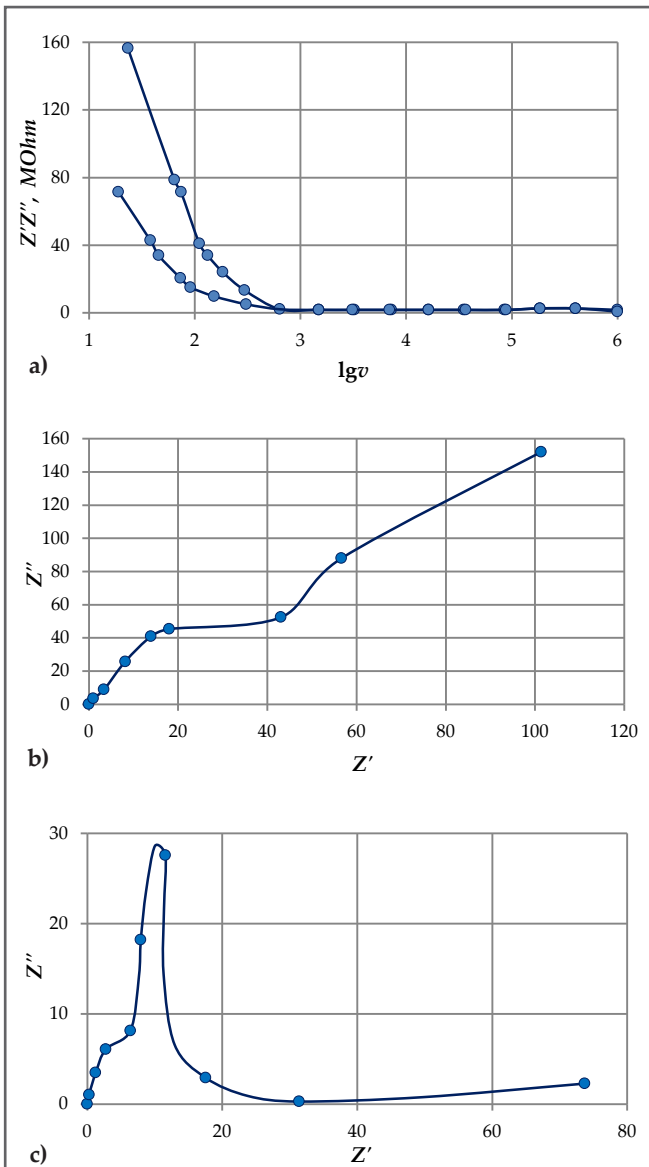


Fig. 2. Frequency dependences of the parameters  $Z'$  and  $Z''$  (a) and Nyquist diagrams for samples of F2ME (b) and F2ME+10% PKR-3M (c)

high frequencies and linear at low frequencies.

The results of the study of the dependence of electrical resistivity  $\rho_v$  at direct current on the volume fraction of graphite ( $\Phi$ )  $\rho_v = f(\Phi)$  are shown in figure 3. This is a monotonically decreasing curve with a clear percolation limit. An increase in  $\Phi$  to 8% leads to a sharp decrease in  $\rho_v$  (increase in electrical conductivity) near the percolation limit (6%) (the specific electrical resistivity of pure PVC  $\rho_v = 2 \cdot 10^{13}$  Ohm·m decreases to  $2 \cdot 10^2$  Ohm·m for PVC + 8% Gr). The value of percolation limit was found as the point of intersection of the lines corresponding to the minor axis and the descending part of the characteristic.

The found value of  $\Phi_p = 6.35\%$  for the value of the leakage limit in the inhomogeneous system we investigated corresponds to the value found in [2] for suitable systems and agrees well with the known provisions of the theory of electrical conductivity leakage.

The graph consists of three parts: the high-Ohmic part  $0 \leq \Phi \leq 4$  (part I), where the resistance is determined by the matrix resistance;  $4 \leq \Phi \leq 6$  section (part II), where the maximum change of  $\rho_v$  where the composite resistance is no longer determined by the resistance of either the matrix or the conductive filler, and the section where the dependence  $\lg \rho_v = f(\Phi)$  is weakly expressed (part III). In this section the composite resistance  $\rho_v$  is determined by the conductor resistance. In part I, most of the conductive particles are isolated from each other by a dielectric layer. When the filler volume fraction exceeds 8%, the level of electrical conductivity is due to the network of conductive channels (clusters) formed in the volume of the polymer matrix.

According to percolation theory, the electrical conductivity of the composite for the state  $\Phi > \Phi_p$  is basically determined

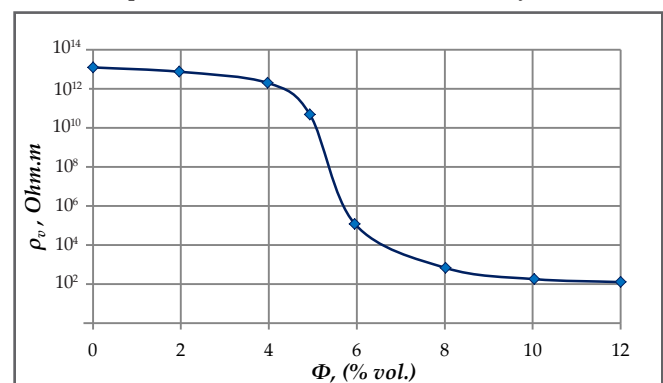


Fig. 3. Dependence of  $\rho_v$  on graphite concentration for PVC+Gr composites

by the following universal law:

$$\sigma_k = \sigma_f (\Phi - \Phi_p) t. \quad (6)$$

Here  $\sigma_f$  and  $\Phi$  – are conductivity and volume concentration of the conductive filler, respectively,  $\sigma_k$  – is conductivity of the composite,  $\Phi_p$  – is percolation limit and  $t$  – is the critical index.

For the case  $\Phi < \Phi_p$  the change in the true part  $\varepsilon'$  of the complex permittivity of the composite near the percolation limit obeys the law (1):

$$\varepsilon' = \varepsilon_M \left| \frac{\Phi_M - \Phi}{\Phi_p} \right|^{-s} \quad (7)$$

Here,  $\varepsilon_M$  – dielectric permittivity of the matrix,  $s$  – is the critical index. Critical indexes  $t$  and  $s$  are universal parameters (composites) and allow to determine specific conductivity and dispersion of dielectric permittivity.

Figure 4a shows how the dielectric permittivity of the PVC-Gr composite system changes when the volume concentration of graphite  $\varepsilon'$  changes.

A sharp increase in dielectric permittivity  $\varepsilon' = 214$  is observed when the volume fraction of graphite is 6%. This is 35 times greater than the dielectric permittivity of the PVC matrix (the dielectric permittivity of pure PVC is  $\varepsilon' \approx 6$ ).

Such a large dielectric permittivity estimate near the percolation concentration can be explained by the diamond mini-capacitor effect. Mini-capacitors consist of different layers of graphite separated by a thin insulating layer of polymer matrix. Such materials are used in high-voltage insulation structures, power capacitors, etc. are used as additional layers regulating the area distribution.

Another reason for the increase in  $\varepsilon'$  composite with increasing  $\Phi$  (graphite concentration) is the Maxwell-Wagner-Sillars (MVS) effect, which occurs when an external electric field is applied after the conductive phase has stabilized in

the dielectric phase. The MVS relaxation mechanism is due to the boundary polarization phenomenon that exists in a heterogeneous system consisting of phases with different dielectric permittivities ( $\varepsilon'$ ) and electrical conductivities ( $\sigma$ ). Such composite materials with high dielectric permittivity are used in energy-efficient electrical equipment.

It is known that the energy density in a flat capacitor is defined by the formula  $W = \varepsilon' \varepsilon_0 E^2 / 2$ . Here  $\varepsilon$  – is dielectric permittivity,  $\varepsilon_0$  – is dielectric permittivity ( $\varepsilon_0 = 8.85 \cdot 10^{-12}$  F/m),  $E$  – is applied external field strength. If it is necessary to apply an electric field of  $1.37 \cdot 10^5$  V/m to obtain an energy density of  $0.5$  J/m<sup>3</sup> in a capacitor using pure PVC as the insulating material between the plates, when using PVC + 6% Gr composite with dielectric constant of 214 as insulation, it is enough to apply a field strength of  $2.3 \cdot 10^4$  V/m to obtain the same energy.

From figure 4b shows that the value of  $\text{tg}\delta$  also increases with growth  $\Phi$ . As a result of formation of conducting grids (clusters) around percolation limit ( $\Phi \geq \Phi_p$ )  $\text{tg}\delta$  increases by several orders of magnitude. The tangent of the dielectric loss angle of the composite system PVC+10% Gr was  $1.1 \cdot 10^2$  at 1 kHz. This is 2345 times the dielectric loss (0.0469) of a pure PVC matrix. Such composites are not suitable for use in power-consuming devices because of the large dielectric losses.

In figure 4 shows that in the PVC/Gr composite system, a sharp transition from dielectric to conductor occurs at room temperature (20 °C) as the concentration of graphite increases. The increase in DC conductivity ( $\sigma_{DC} = 1/\rho_0$ ) with the increase in Gr concentration can be explained by an increase in the concentration of charge carriers. In this case the filler particles (Gr) can be considered as a point source of heat carriers. In the percolation limit the DC conductivity of composites is very small and they have typical dielectric properties.

Frequency dependences of  $\sigma_{AC}$ ,  $\varepsilon'$  and  $\text{tg}\delta$  of PVC/Gr composites of different concentrations measured at room temperature are shown in figure 5(a), 5(b) and 5(c). Figure 5(a) shows the dependence of  $\sigma_{AC}$  conductivity on the electric field frequency in double logarithmic scale.

A common feature of all dependencies is a linear increase in conductivity with increasing frequency. This shows the surface dependence of  $\sigma_{AC}$  ( $\sigma_{AC} \sim f^n$ , where  $n$  is the parameter or critical index determined by the conduction mechanism). This nature of the  $\sigma_{AC}$  frequency dependence indicates a stepwise charge transfer mechanism and is characteristic of dielectric materials. The dependence  $\sigma_{AC}(f)$  of PVC compensates for the dependence  $\sigma_{AC} \sim f^n$ . Here  $n \approx 0.56$ . For composite samples with graphite content of 1 and 2 % the transition region (region I) of conductivity above 500 and 1000 Hz is passed from relatively strong ( $n \approx 0.39$  and  $n \approx 0.37$ ), respectively, to the relatively weak field ( $n \approx 0.48$  and  $n \approx 0.46$ ). In all cases the critical index  $n$  satisfies the condition  $0 < n < 1$ , which is an indicator of the jump-barrier mechanism of AC conductivity. According to this mechanism, electron jumps occur at localized levels around the Fermi level [3-5]. The figure shows that the critical value of the frequency  $f_{cr}$  (the frequency at which the transition from region I to region II occurs) shifts toward higher frequencies as the graphite concentration increases.

Note that AC conductivity of the studied samples is significantly greater than their DC conductivity (measured

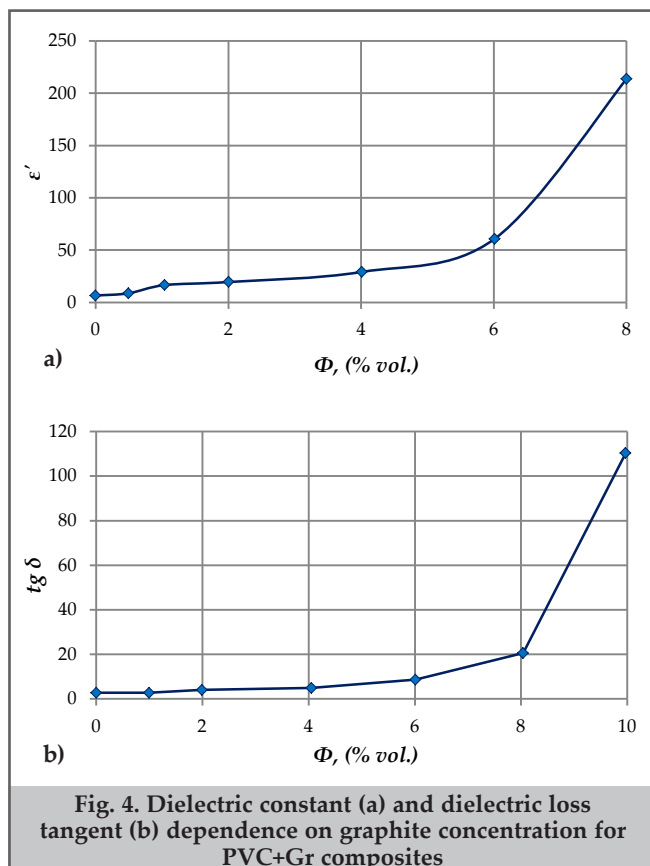
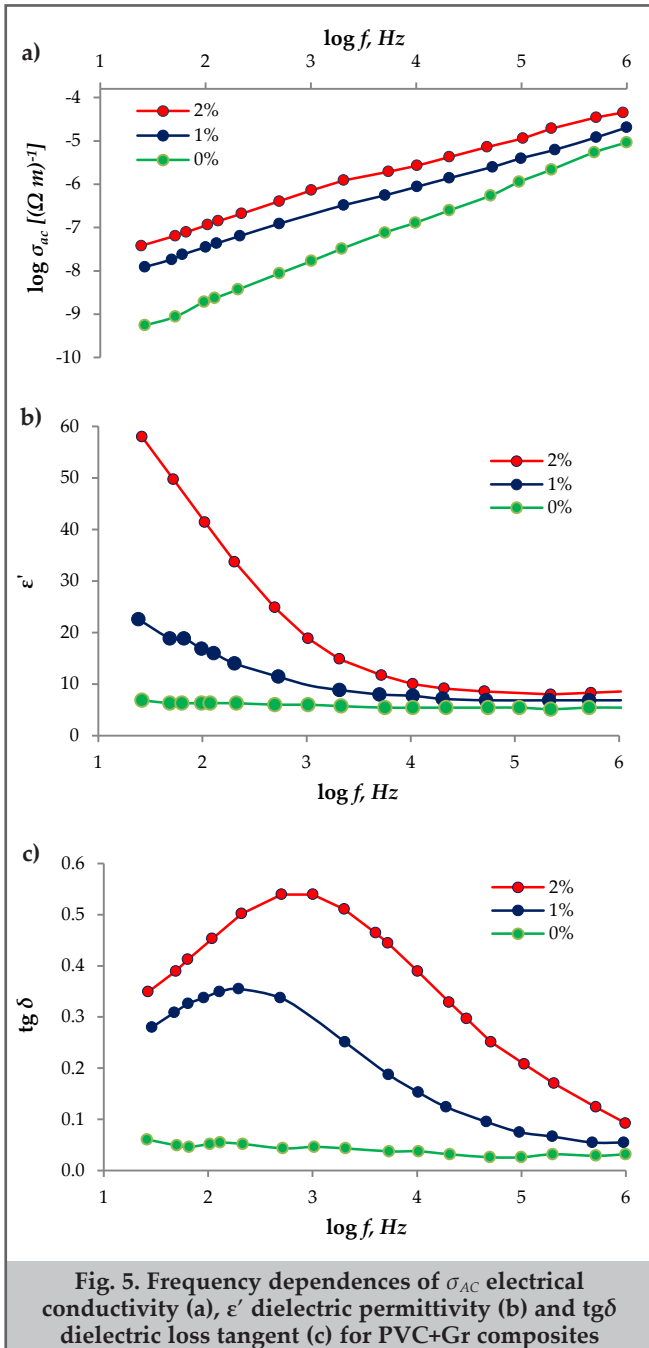


Fig. 4. Dielectric constant (a) and dielectric loss tangent (b) dependence on graphite concentration for PVC+Gr composites



**Fig. 5. Frequency dependences of  $\sigma_{AC}$  electrical conductivity (a),  $\epsilon'$  dielectric permittivity (b) and  $\text{tg}\delta$  dielectric loss tangent (c) for PVC+Gr composites**

at room temperature), because it consists of the sum of relaxation part ( $A\omega^n$ ) due to two components – the volume electrical conductivity (usually coinciding with the DC conductivity and determined by carrier migration) and frequency generated dielectric dispersion.

The second component is determined by a set of relaxation processes at the polymer-filler-phase interface:

$$\sigma_{AC} = \sigma_{DC} + A\omega^n, \quad (8)$$

Here,  $\omega = 2\pi f$  is angular frequency,  $A$  – is a temperature-dependent constant.

Let's look at the results of changes in the complex dielectric constant and dielectric losses of PVC and its composites. The dependencies of  $\epsilon'(f)$  and  $\text{tg}\delta(f)$  are shown in figure 3 (b-c). It seems that the value of  $\epsilon' = 6$  for PVC in the studied frequency range is practically independent of the frequency. The frequency variance of the dielectric constant is observed for samples of 1 and 2% with a concentration increase, but none of the mechanisms of dielectric relaxation

is manifested at these frequencies, as none of the characteristic peaks observed in the dependence can be associated with a particular type of molecular mobility.

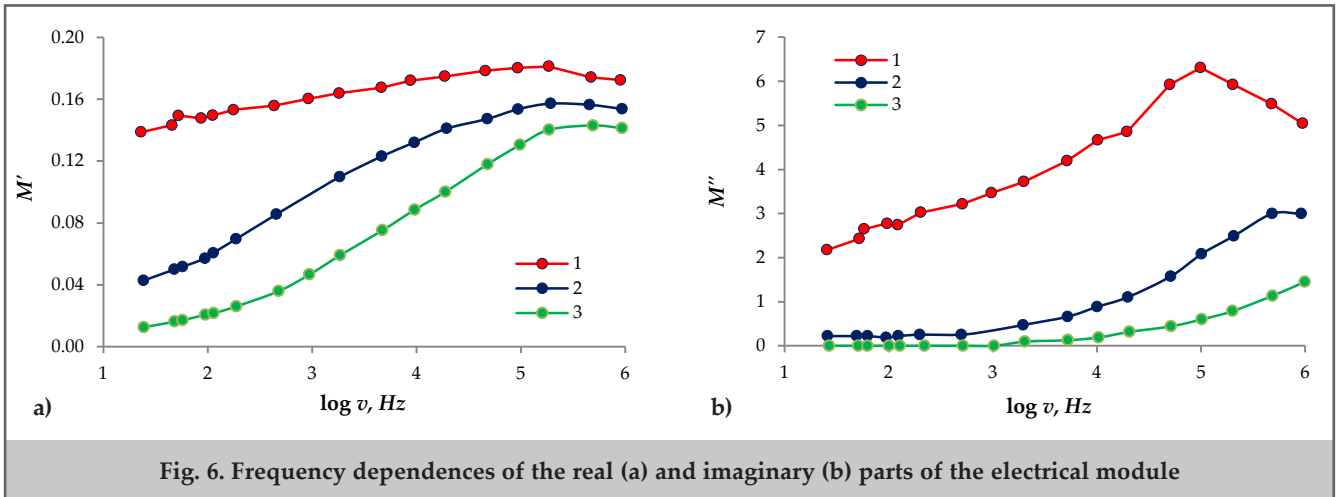
It has large values of  $\epsilon'$  at low frequencies and decreases exponentially with increasing frequency. The concentration and frequency dependences of  $\epsilon'$  are stronger in the low frequency range ( $f < 10^3$  Hz). The large value of  $\epsilon'$  in the low-frequency region is due to the increase in interfacial polarization. This type of polarization is explained by the difference in the cost of conductivity of the matrix and micro- and nanoparticles. Phase polarization is always present in heterogeneous composites because the charge carriers move towards the interfacial boundary under the influence of the external field [6-8] and mainly affect the dielectric properties at low frequencies ( $25 \cdot 10^4$  Hz).

As the frequency decreases, the time required for drift of the carriers increases and the value of the dielectric constant increases. The described decrease in  $\epsilon'$  with increasing frequency reflects the difficulty of orientation of dipoles with increasing periodic rate of change of the applied field. As the filler concentration increases (and the frequency decreases), the dielectric loss ( $\epsilon''$ ) also increases as  $\epsilon'$ . Note that the sharp increase in  $\epsilon''$  at low frequencies is due to the conduction process. The peak dependence of  $\epsilon''$  indicates that a relaxation process has taken place in the system. On the other hand, the described increase in  $\epsilon'$  with decreasing frequency is an indication of the predominance of the binding role of the electrodes at low frequencies. Dielectric properties at low frequencies are determined by electrode polarization. At high frequencies, the dielectric properties are not determined by electrode polarization. As the frequency increases, the dipoles cannot rotate fast enough, and thus their oscillation lags behind the field oscillation. During the subsequent increase in frequency, the dipoles almost do not feel the electric field, and the orientation polarization stops, and the dielectric constant, which decreases at higher frequencies and remains practically constant, is conditioned only by boundary polarization. At low frequencies, the value of  $\epsilon''$  increases as the concentration of graphite microparticles increases. This is due to the fact that the interaction between the polymer chains and microparticles increases, the structure of the composites becomes more regular, and the volume loads accumulate at the interfacial boundary. Such accumulation of volumetric loads leads to an increase in dielectric losses due to the capture of virtual loads at the interfacial boundary of multicomponent materials with different conductivities.

When the frequency of the external electric field varies from 25 Hz to  $10^6$  Hz, the rate of reduction of  $\epsilon'$  increases with increasing graphite concentration from 1 to 2%, and  $\epsilon'$  decreases by about 7.3 times for PVC + 2% Gr. The parameter  $\Delta\epsilon = (\epsilon_s - \epsilon_\infty)$ , which expresses the full width of the variance (where  $\epsilon_s$  and  $\epsilon_\infty$  are the dielectric constants at low and high frequencies, respectively) is equal to 50.41.

The frequency dependence of  $\text{tg}\delta$  for PVC+Gr composites is shown in figure 3 (c).

It seems that in this case, the  $\text{tg}\delta$  of pure PVC remains practically constant in the entire frequency range, but the  $\text{tg}\delta$  of the composites with graphite concentrations of 1 and 2%, respectively, increases to 200 and  $10^3$  Hz, exceeds the maximum and then increases the frequency scale. decreases to the end. Believe that the increase in the conductivity of the composites and the consequent increase in  $\text{tg}\delta$  is due



to the increase in the concentration of free-charge electrons from levels near the Fermi level, even at room temperature, as a result of thermoelectron emission to local levels in the composite restricted zone. The decrease in  $\text{tg}\delta$  is due to the fact that as the frequency increases, the electron oscillation weakens under the influence of the opposite field, and the resulting load system gradually collapses.

It is known that the results of dielectric measurements can be analyzed by the formalisms of dielectric constant, electrical modulus and AC – electrical conductivity. The complex electrical modulus  $M$ , which is equal to the inverse of the complex dielectric constant, is found using the formula (9):

$$M = \frac{1}{\epsilon} = \frac{1}{\epsilon' - j\epsilon''} = \frac{\epsilon'}{\epsilon'^2 - \epsilon''^2} + j \frac{\epsilon''}{\epsilon'^2 - \epsilon''^2} = M' + jM'' \quad (9)$$

Here,  $\epsilon'M'$  and  $\epsilon''M''$  – are the real and imaginary parts of the dielectric constant and electrical module, respectively.

The real and imaginary parts of the electrical module are determined as follows:

$$M' = \frac{1}{\epsilon'^2 - \epsilon''^2} \quad \text{and} \quad M'' = \frac{\epsilon''}{\epsilon'^2 - \epsilon''^2} \quad (10)$$

Since the relaxation effects in metal-dielectric and semiconductor-dielectric systems are mainly due to cross-border polarization processes, they are presented and studied in the form of electrical modulus as a function of frequency, temperature and concentration of fillers. The interpretation of the relaxation event in electrical modulus formalism has the advantage over other methods in that the dielectric constant at low frequencies and high temperatures and the variation over a wide range of dielectric losses are minimized.

In addition, in this case, the nature of the electrode, the electrode-sample contact, the injection of charges and the difficulties with the absorbed additives can be ignored. In polymer matrix composites, the relaxation effects are conditioned by boundary effects, phase transitions, and polarization or conduction mechanisms. The dielectric characteristics of the studied samples have already been expressed through the real and imaginary parts of the dielectric constant. Now let's express these characteristics in the formalism of the electrical module.

Figures 6a and 6b show the frequency dependencies of the real (a) and imaginary (b) parts of the complex electrical module, respectively, for the samples studied.

The figures show that the  $M'$  and  $M''$  values increase with increasing frequency (up to 2·10<sup>5</sup> Hz) and then decrease.

The fact that  $M'$  and  $M''$  exceed the maximum at a certain frequency indicates that there is a process of relaxation to pure PVC, and the amplitude of the peaks decreases as the concentration of Gr microparticles increases. It is well known that  $\alpha$ -relaxation is associated with a glass-rubber phase transition. When enough heat energy is supplied to the polymer, most of the amorphous macromolecular chains relax at the same time and participate in the cooperative action.

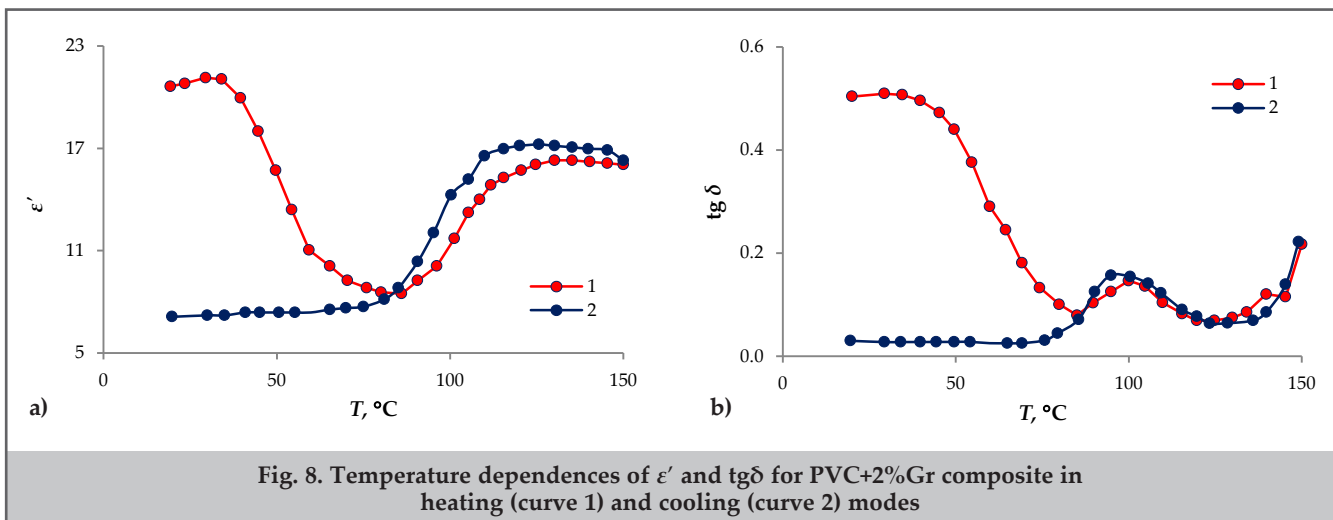
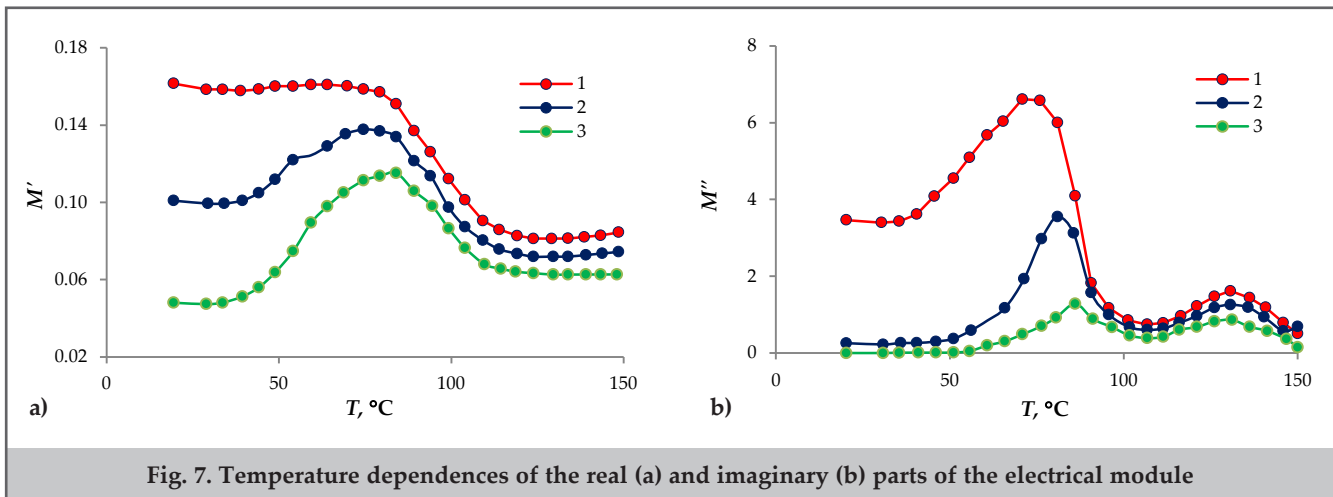
In polymer matrix composite systems, the glass transition is determined by the chemical structure of the polymer chains and, in many cases, the type of additive. As a rule, the temperature at which the loss peak corresponding to  $\alpha$  relaxation in the dielectric spectrum at a constant frequency is taken as the glass transition temperature.

Figure 7a shows the change in  $M'$  with increasing temperature for these samples. The  $M'$  real part of the  $M^*$  complex electrical module of pure PVC remains constant up to the glazing temperature (800) and then decreases sharply. Pure PVC does not show any peaks.  $M'$  does not change up to 400 for the composite samples and then shows a wide peak in the temperature range 40-115 °C.

This course of the  $M' = f(T)$  function of the composites is characteristic of them and is associated with the  $\alpha$  relaxation process in pure PVC. After 85 °C, the real part of the complex module decreases for all samples and remains constant in the range of 115-150 °C.

Figure 7b shows the temperature dependence of the  $M''$  loss modulus index at constant frequency (10<sup>3</sup> Hz) for all studied samples. Here, two relaxation processes are clearly visible at low (70-86 °C) and relatively high (130 °C) temperatures. The characteristic relaxation for PVC is formed near the peak phase transition (70 °C), and for PVC + 2% Gr at 85 °C. As can be seen, both temperatures are close to the glazing temperature of pure PVC. This indicates that the relatively weak dielectric relaxation process corresponds to the glass-rubber phase transition. Peak intensity decreases with increasing Gr concentration. On the other hand, an increase in the Gr concentration causes the temperature of the first peak to shift from 70 °C to 85 °C in the high temperature range. For all samples, the second maximum temperature (130 °C) in the temperature dependence does not depend on the concentration of Gr.

Figure 8(a, b) shows the change in the real part  $E'$  and  $\text{tg}\delta$  of the complex dielectric constant  $\epsilon$  for PVC + 2% Gr samples in the heating-cooling mode at a speed of 3 degrees/minute.



The value of  $\epsilon'$  increases slightly until the temperature reaches 35 °C, then decreases sharply, exceeds the minimum at the glassing temperature of PVC (80 °C), and then again increases up to 125 °C. The value of  $\epsilon'$  remains constant in the range (125-150) °C.

During heating, the value of  $\epsilon'$  is higher than during cooling. The thermal properties of the samples  $\epsilon'$  and  $\text{tg}\delta$  often overlap with the heating curves during the temperature dependence of the cooling process in the high temperature phase of the samples  $\epsilon'$  and  $\text{tg}\delta$  up to 80 °C. The temperature hysteresis effect is present at  $T < 80$  °C, and the values of  $\epsilon'$  and  $\text{tg}\delta$  are lower during heating than during cooling. As a result of the heating-cooling cycle, the dielectric properties of the samples take on a new value and tend to stabilize at  $T < 80$  °C in the opposite process. Finally,  $\epsilon'$  and  $\text{tg}\delta$  must return to their previous values. The price at this point was 7.27 and 0.035, and the values before the start of the thermal cycle were 20.67 and 0.057, respectively. This property of the composite material is due to the thermally stimulated process of redistribution of loads at the particle-matrix boundary. Composite samples can remain in this state for a long time after cooling to room temperature. This property of composite materials causes hysteresis events based on the effect of «asymmetry» of temperature rise of electroactive defects.

The dependence of  $\text{tg}\delta = f(T)$  (fig. 8b) has the following specific characteristics: The properties of the function  $\text{tg}\delta = f(T)$  up to a temperature of 80 °C are almost similar to the properties of the function  $\epsilon' = f(T)$ , and the value of  $\text{tg}\delta$

of the composites where remains approximately constant is twice as short as pure PVC. The condition of the observed maximum and minimum of  $\text{tg}\delta$  at  $T = 100$  and 130 °C, respectively, does not depend on the amount of graphite in the matrix. During the heating-cooling period, the relative changes in temperature at  $\epsilon'$  and  $\text{tg}\delta$  were approximately 33% and 61%, respectively.

Electrophysical properties are characterized by the value of electrical resistance, electrical strength (strength in perforation), dielectric constant and dielectric loss. The value of these characteristics and their dependence on aggressive factors (especially moisture absorption), temperature and frequency of the electric field determine the choice of PVC – based insulation composites. Therefore, it is of practical interest how the electrophysical properties of polymer composites change after exposure to water. For this purpose, the electrophysical parameters of pure PVC and PVC + 2% Gr composite samples were measured even after they were stored in water.

Based on the results obtained, graphs of the dependence of specific volume electrical resistance ( $\rho_v$ ), dielectric constant ( $\epsilon$ ) and dielectric loss tangent ( $\text{tg}\delta$ ) on the retention time of the samples in water at  $T = 273$  K (fig. 9a,b,c) were constructed.

The analysis of the results allows to identify the parts of the scale where more dynamic changes of electrophysical parameters are observed. A significant decrease in the parameter  $\rho_v$  (specific volume electrical resistance), as well as an increase in  $\text{tg}\delta$  (tangent angle of dielectric loss) and

$\varepsilon$  (dielectric constant) occur before the samples remain in water for 8 hours. The subsequent water retention process of the samples ( $\tau > 8$  hours) has little effect on the change of the mentioned characteristics of the polymer composites. They remain almost stable.

It should be noted that these measurements are due to the fact that the properties of insulation materials are highly dependent on the amount of water in them. The sensitivity of the composites to moisture is of great importance because the absorbed water is significant in the composite material and may cause irreversible changes.

This result confirms the idea that such a change in the values of  $\rho_v$ ,  $\varepsilon'$  and  $\text{tg}\delta$  is characteristic for all types of PVC composites designed for insulation of cable products.

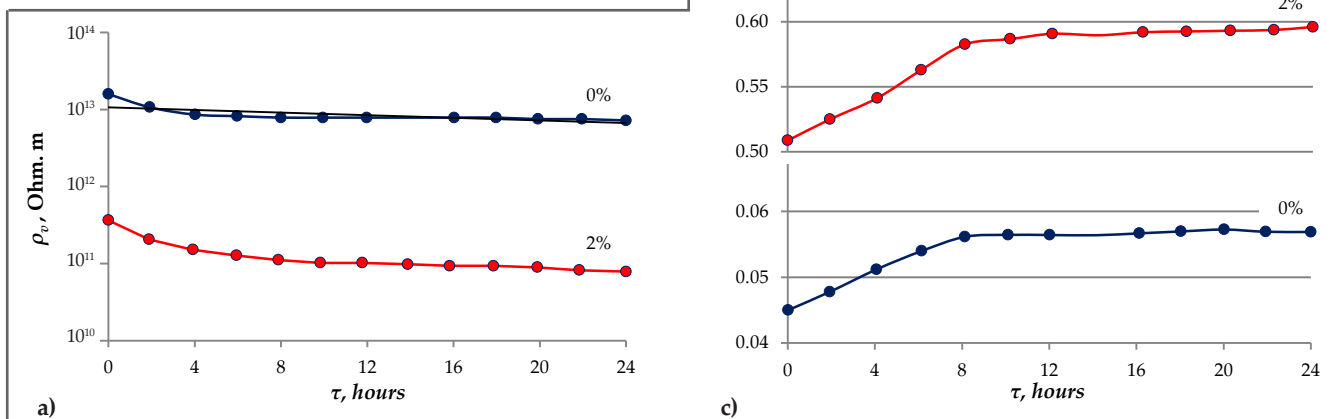


Fig. 9. Dependence of  $\rho_v$  (a),  $\varepsilon'$  (b) and  $\text{tg}\delta$  (c) on water retention time  $\tau$  for PVC and PVC+2%Gr composite

## Conclusions

HDPE/PKR-3M 0-3 composites prepared by the mixing and the hot compression mold technique has been investigated by ACIS. The frequency dependence of the real and imaginary parts of the impedance and the Cole-Cole plot is analyzed. Future work will be related to full impedance measurements at different frequencies, analysis of the real and imaginary part behaviors and the relation to the polarization processes in the ferroelectric film.

## References

- Pandey, M., Joshi, G. I., Deshmukh, K., Ahmed, J. (2015). Impedance spectroscopy and conductivity studies of CdCl<sub>2</sub> doped polymer electrolyte. *Advanced Materials Letters*, 6(2), 165-171.
- Senthil, V., Bahapanda, T., Kumar, S. N., et al. (2012). Relaxation and conduction mechanism of PVA:BYZT polymer composites by impedance spectroscopy. *Journal of Polymer Research*, 19, 9838.
- Khan, I., Saeed, K., Khan, I. (2019). Nanoparticles: properties, applications and toxicities. *Arabian Journal of Chemistry*, 12(7), 908-931.
- Kidalov, S. V., Shakhov, F. M., Vul, A. Y. (2008). Thermal conductivity of sintered nanodiamonds and microdiamonds. *Diamond and Related Materials*, 17(4), 844-847.
- Kirsh, I. A., Pomogova, D. A., Sogrina, D. A. (2013). Biodecomposed polymeric compositions on the basis of agriculture's waste / in «Progress in organic and physical chemistry». *Apple Academic Press*.
- Kochetov, R. (2011). Modeling of the thermal conductivity in polymer nanocomposites and the impact of the interface between filler and matrix. *Journal of Physics D: Applied Physics*, 44(39), 1-12.
- Kurbanov, M. A., Aliev, Kh. S., Kerimov, E. A., Sultanakhmedova, I. S. (2009). Plasma crystallization of polymer-ferroelectric/piezoelectric ceramic composites and their piezoelectric properties. *Physics of the Solid State*, 51(6), 1223-1230.
- Kurbanov, M. A., Aliyev, H. S., Allahverdiyev, Z. A., Niftiyev, S. N. (1997). Influence of the polarity of the polymer matrix on thermal, electric and mechanical properties of composites on the basis of polymers-nitrides and carbides of metals. In: *Elektrik-Elektronik Bilgisayar Muhendisligi 7 Ulusal Kongresi, Turkiye, Ankara*.

## **Импедансная спектроскопия полимерно-керамических композитов**

*Х. С. Алиев, Х. В. Фаттаев*

Азербайджанский технический университет, Баку, Азербайджан

### **Реферат**

Композиты HDPE/PKR-3M 0-3, приготовленные методом смешивания и горячего прессования в пресс-форме, были исследованы с помощью ACIS. Анализируется частотная зависимость действительной и мнимой частей импеданса и график Коула-Коула. Будущая работа будет связана с измерениями полного импеданса на различных частотах, анализом поведения действительной и мнимой частей и связи с поляризационными процессами в ферроэлектрической пленке.

**Ключевые слова:** полимерный композит, импедансная спектроскопия, полимер, комплексное сопротивление, электрическое поле, время релаксации, угол сдвига фаз.

## **Polimer-keramik kompozitlərin impedans spektroskopiyası**

*H. S. Əliyev, H. V. Fattayev*

Azərbaycan Texniki Universiteti, Bakı, Azərbaycan

### **Xülasə**

Qarışdırılma və pres-formada isti preslənmə metodu ilə hazırlanmış HDPE/PKR-3M 0-3 kompozitləri ACIS köməyi ilə tədqiq edilmişdir. İmpedansın həqiqi və xəyali hissələrinin tezlik asılılığı və Koul-Koul qrafiki analiz edilmişdir. Gələcək işlərimiz müxtəlif tezliklərdə tam impedansın ölçülməsi, həqiqi və xəyali hissələrin analizi və ferroelektrik təbəqədə polyarlaşma prosesləri ilə əlaqədar olacaqdır.

**Açar sözlər:** polimer kompozit, impedans spektroskopiyası, polimer, kompleks müqavimət, elektrik sahəsi, relaksasiya müddəti, fazaların sürüşmə bucağı.